ACCOUNTS
of chemical research

Tuning Molecular Orbitals in Molecular Electronics and Spintronics

WOO YOUN KIM AND KWANG S. KIM*

Center for Superfunctional Materials, Department of Chemistry, Pohang University of Science and Technology, Pohang 790-784, Korea

RECEIVED ON MAY 21, 2009

CONSPECTUS

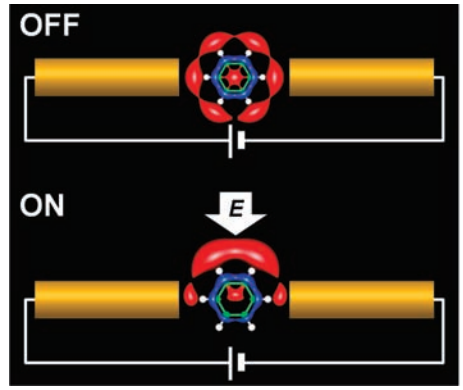

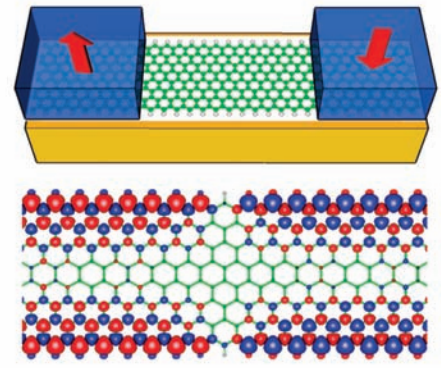

With the advance of nanotechnology, a variety of molecules, from single atoms to large-scale structures such as graphene or carbon nanotubes, have been investigated for possible use as molecular devices. Molecular orbitals (MOs) are a key ingredient in determining the transport properties of molecules, because they contain all the quantum mechanical information of molecular electronic structures and offer spatial conduction channels for electron transport. Therefore, the delicate modulation of the MOs enables us to tune the performance of electron transport through the molecule. Electric and magnetic fields are powerful and readily accessible means for that purpose. In this Account, we describe the effects of external fields on molecular electronic and spintronic devices.

Quantum transport through a molecule that connects source and drain electrodes depends strongly on the alignment of molecular energy levels with respect to the chemical potentials at both electrodes. This dependence results from the energy levels being exploited in resonant tunneling processes when the molecule is weakly coupled to the electrodes in the molecular junction. Molecular energy levels can be shifted by the Stark effect of an external electric field. For a molecule with no permanent dipole moment, the polarizability is the primary factor determining the energy shift of each MO, according to the second-order Stark effect; more polarizable MOs undergo a larger energy shift. Interestingly, even a small shift may lead to a completely nontrivial result. For example, we show a magnetic on−off switching phenomenon of a molecule controlled by an electric field. If a molecule has a nonmagnetic ground state but a highly polarizable magnetic excited state with an energy slightly above the ground state, the magnetic excited state can have lower energy than the ground state under a sufficiently strong electric field.

A magnetic field is normally used to control spin orientation in a ferromagnetic system. Here we show that the magnetic field can also be used to control MOs. A graphene nanoribbon with zig-zag-shaped edges (ZGNR) has a ferromagnetic spin ordering along the edges, and the spin states have unique orbital symmetries. Both spin polarizations and orbital symmetries can simultaneously be controlled by means of an external magnetic field. The ZGNR spin-valve devices incorporating this effect are predicted to show an extreme enhancement (compared with conventional devices) of magnetoresistance due to the double spin-filtering process. In such a system, spins are filtered not only by spin matching−mismatching between both electrodes as in normal spin-valve devices, but also by the orbital symmetry matching−mismatching. Thus, a new type of magnetoresistance, and with extremely large values, so-called super-magnetoresistance (distinct from the conventional tunneling or giant magnetoresistance), is available with this method.

MOs are at the heart of understanding and tuning transport properties in molecular systems. Therefore, investigating the effects of external fields on MOs is important not only for understanding fundamental quantum phenomena in molecular devices but also for practical applications in the development of interactive devices.

Published on the Web 09/21/2009 www.pubs.acs.org/acr
10.1021/ar900156u

Introduction

The fancy idea of utilizing single molecules as an individual electronic device[1] is no longer an unreachable task with the advent of modern nanotechnology. For the past decade, much effort has been devoted to devising experimental methods to fabricate reliable molecular devices[2−5] and to developing theoretical tools to understand quantum phenomena observed in the devices.[6−8] As a result, molecular electronics and spintronics have firmly settled down as a new active field in chemistry, physics, and materials science.[9−12] However, there are still many issues to be resolved to take a leap toward the ultimate aim of the new field to complement or replace conventional electronics. One of the issues would be the design of interactive devices whose transport characteristics can be manipulated by an external means.

In molecular devices, the role of molecular orbitals (MOs) is crucial in determining their quantum mechanical transport properties, since the MOs contain all quantum mechanical information on the electronic structure of the molecule and further provide a spatial region where traversing electrons pass through and interact with each other. Hence, external manipulation of MOs must be a direct way to tune transport properties of a molecule. Questions arising at this point would be "what is a useful means to control MOs?" and "how does it work?". The answers for these questions would depend on the purpose or function of a device. Figure 1 shows exemplary molecular devices controlled by an external means. Electric or magnetic fields are typical means to change the energy levels of MOs by controlling their charges or spins, respectively. An optical field could also be used to manipulate MOs.[13] These external fields enable us to design a molecular switching device where "ON" and "OFF" are controlled by an external field, as shown in Figure 1. It is particularly interesting to note that the MOs of a host molecule are sensitively influenced in their shapes and energies when the host molecule is contacted through either covalent or noncovalent bonding by a guest atom or molecule.[8] This effect can be used to design an ultrasensitive sensor to be able to detect even a single atom or molecule.

To understand the transport properties, we have been investigating the effects of electric and magnetic fields on MOs using theoretical methods. Indeed, we note that the effects are critical in the design of molecular devices. Moreover, under certain conditions, such field effects often result in unusual phenomena useful for exotic devices. The goal of this Account is to offer insights into the role of MOs in quantum transport through molecular devices, to explain the effects of external fields on MOs, and to describe how to utilize such effects for the design of novel molecular devices.

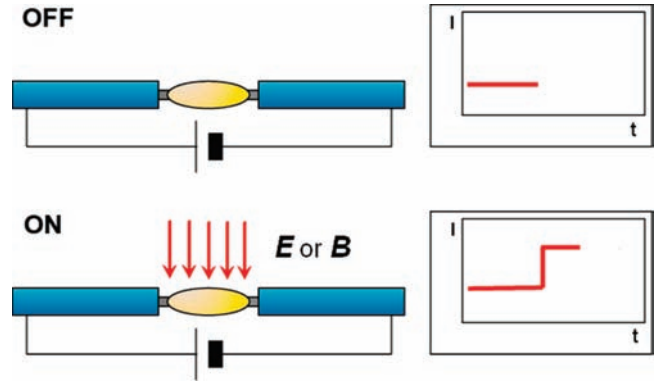

FIGURE 1. Schematics of a molecular switching device controlled by external electric (**E**) or magnetic (**B**) fields.

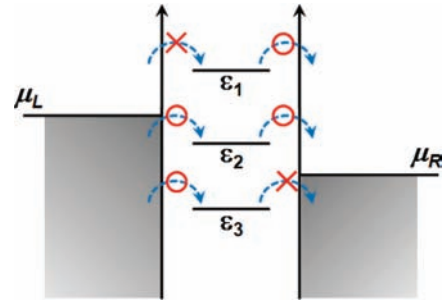

FIGURE 2. Schematic energy level diagram of a molecule with contacts. ε_1, ε_2, and ε_3 denote molecular energy levels, and μ_L and μ_R are the chemical potentials of the left and right electrodes. The difference between two chemical potentials equals an applied bias voltage (V_b), $\mu_L - \mu_R = V_b$.

Quantum Transport in Molecular Devices

Let us consider a nanoelectronic device comprised of a molecule connected between two electrodes as shown in Figure 1. Electrical currents (I) are driven by a bias voltage (V_b) applied to the molecular junction. For a short molecule, electron transport occurs through the energy levels of the molecule in the resonant tunneling regime when the molecule-lead coupling is low. From the spatial point of view, MOs corresponding to the energy levels are the conducting channels. Thus, it is essential to understand the role of MOs for quantum transport in molecular devices and furthermore to manipulate them for designing novel devices. To facilitate our discussion, we briefly describe qualitative and quantitative features for quantum transport in molecular junctions with a schematic model to provide a physical insight. The details of concrete description are available in more specialized literature.[14−27]

Figure 2 shows possible occasions of electron transport, which does not involve energy change due to electron−phonon or electron−electron interactions in the tunneling pro-

cess. For the energy level ε_1, electron tunneling is not allowed, because there is no electron at the energy ε_1 of the left (source) electrode. For the energy level ε_3, transport is completely blocked due to the Pauli exclusion principle, because all states of the right (drain) electrode at the energy ε_3 are fully occupied. Therefore, only the energy level ε_2 located between the two chemical potentials (μ_L and μ_R) at both electrodes can contribute to the electrical currents. Thus, the first factor in determining currents is the relative alignment of MO energy levels to the chemical potentials at both electrodes.

The second factor must be the extent of transmission for each conducting channel. If a MO is spatially delocalized around the molecular geometry and well coupled to the incoming/outgoing states in the source/drain electrodes, the transmission probability through the MO should be high. In contrast, the transmission probability for a localized MO should be low because this MO weakly couples with the incoming/outgoing states of both electrodes. Strong electron−electron and electron−phonon interactions cause more complex scattering processes, but these factors are important in the incoherent tunneling regime, which we do not discuss here. Consequently, in most cases, (spin-dependent) currents are obtained using the following equation:

$$I_\sigma = \frac{e}{h}\int T_\sigma(\varepsilon)\{f(\varepsilon-\mu_L) - f(\varepsilon-\mu_R)\}\,\mathrm{d}\varepsilon \tag{1}$$

where $T(\varepsilon)$ is the transmission (probability) of an electron with spin σ as a function of energy ε, e is the electron charge, h is the Planck constant, and $f(\varepsilon)$ is the Fermi distribution function. The energy range where electron transport is allowed, the so-called current window, is set up by the difference of two Fermi functions in eq 1.

The spin-dependent transmission is given by the Fisher−Lee relation:[14,24]

$$T_\sigma(\varepsilon) \equiv \mathrm{Tr}\left[\mathrm{Im}\left(\sum\nolimits^{r}_{L\sigma}(\varepsilon)\right)G^{r}_{\sigma}(\varepsilon)\mathrm{Im}\left(\sum\nolimits^{r}_{R\sigma}(\varepsilon)\right)G^{a}_{\sigma}(\varepsilon)\right] \tag{2}$$

where $G^a(\varepsilon)$ and $G^r(\varepsilon)$ are the advanced and retarded Green's function and $\sum^r_L(\varepsilon)$ and $\sum^r_R(\varepsilon)$ are the retarded self-energy for the left and right contact. For the case of a usual collinear spin-polarized system, one deals with two spin component matrices, for example, Hamiltonian (H_α and H_β) or density matrix (ρ_α and ρ_β). To describe molecular spintronic devices involving a magnetic domain wall, however, one should deal with a spin vector to represent an arbitrary direction. In this noncollinear spin-polarized case, the Green's function matrix is given by the four spin-component block matrices as follows:

$$\bar{G}^r(\varepsilon) = \begin{bmatrix} G^r_{\alpha\alpha}(\varepsilon) & G^r_{\alpha\beta}(\varepsilon) \\ G^r_{\beta\alpha}(\varepsilon) & G^r_{\beta\beta}(\varepsilon) \end{bmatrix} = \frac{1}{\varepsilon\bar{S} - \bar{H}^r - \bar{\Sigma}^r(\varepsilon)} \tag{3}$$

where

$$\bar{S} = \begin{bmatrix} S & 0 \\ 0 & S \end{bmatrix}$$

$$\bar{H} = \begin{bmatrix} H_{\alpha\alpha} & H_{\alpha\beta} \\ H_{\beta\alpha} & H_{\beta\beta} \end{bmatrix}$$

$$\bar{\Sigma}^r(\varepsilon) = \begin{bmatrix} \Sigma^r_{\alpha\alpha}(\varepsilon) & \Sigma^r_{\alpha\beta}(\varepsilon) \\ \Sigma^r_{\beta\alpha}(\varepsilon) & \Sigma^r_{\beta\beta}(\varepsilon) \end{bmatrix}$$

are the overlap, Hamiltonian, and retarded self-energy matrices, respectively. The block Hamiltonian matrix $H_{\alpha\beta}$ is obtained by using the density functional theory with the four spin component density matrix, which is obtained by

$$\rho_{\alpha\beta} = -\frac{1}{\pi}\mathrm{Im}\int_{-\infty}^{\infty} G^r_{\alpha\beta}(\varepsilon)f(\varepsilon)\,\mathrm{d}\varepsilon \tag{4}$$

The Green's function in the integrand of eq 4 is calculated from the Hamiltonian in eq 3. Thus, fully unconstrained noncollinear spin calculation is achieved in a self-consistent manner within density functional theory.

In this context, one can easily find that delicate manipulation of a molecular device would be realized by tuning MOs (for example, spatial extension, symmetry, or energy), since the change in shape or energy of MOs is directly related to the transmission function [$T(\varepsilon)$]. Electric and magnetic fields must be powerful and easily realizable means to do so. In the following sections, we discuss the effects of such external fields on MOs.

Effect of an Electric Field on Molecular Orbitals

An electric field allows controlled and reversible changes of electronic properties of a target system. For instance, in field-effect transistors the electrical charge carrier density of a conducting channel is controlled by an electric field.[28] Superconductivity of correlated oxide systems can be switched by an external electric field.[29] Recently, the electric field has also been employed to modulate transport properties of novel nanosystems such as quantum dots, carbon nanotubes, and graphene nanoribbons.[30] Since electric fields are a primary choice for an external means to control the electronic structure of a molecular device,[31−35] it is important to investigate the electric field effect in molecular systems.

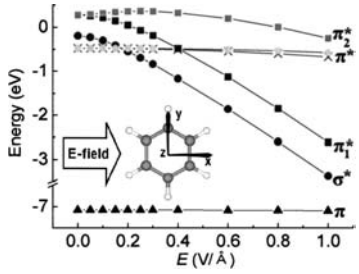

FIGURE 3. Change of frontier orbital energies of the benzene molecule as a function of an applied electric field. Inset shows the direction of the applied field.[35]

An external electric field causes the energy level shift ($\Delta\varepsilon$) of a molecular system:

$$\Delta\varepsilon = -\boldsymbol{\mu} \cdot \mathbf{E} \tag{5}$$

where $\boldsymbol{\mu}$ is the dipole moment and **E** is the electric field. Such an effect depends on characteristics of MOs. If MOs have even symmetry along the direction of the applied electric field, that is, no permanent dipole moment, the MO energy shift proportional to the field due to the first-order (or linear) Stark effect vanishes. Under a strong applied field, however, the MOs are significantly distorted, and thereby their symmetries are broken, resulting in a finite induced dipole moment ($\boldsymbol{\mu}_{\text{ind}} = \alpha\mathbf{E}$, where α is the polarizability). The second-order (or quadratic) Stark effect could drastically change the energy levels of highly polarizable molecules. Thus, the molecular system is controlled by means of an external electric field.

Polarizability is a dominant factor in determining the strength of the Stark effect for a molecule with no permanent dipole moment. Interestingly, each MO in the same molecule has different spatial distributions and thereby different polarizabilities, which means that the energy of a particular MO with high polarizability can distinctively be tuned by an electric field. Figure 3 shows such an example. As a uniform electric field is applied to the benzene molecule, which has no permanent dipole moment, the σ^* and $\pi_1{}^*$ states so sensitively respond that eventually they cross over the degenerate π^* states, which are the lowest unoccupied MOs (LUMOs) at zero bias.[35] In this way, one can tune the alignment of molecular energy levels in the current window by applying an electric field.

Molecular Magnetic Switching Using the Electric Field Effect

Spins are normally controlled by magnetic fields, which are cumbersome to deal with. Spin control can be achieved by an electric field if a device involves energy-dependent (i.e., gate-tunable) spin carriers or strong spin−orbit coupling.[30,36−38] The strong Stark effect that we have discussed above offers a new way to directly control spin states with an electric field for molecular devices. Here we show an example to control magnetic on/off switching with electric fields.

A benzene molecule has 6π electrons, showing a stable structure with resonance energy, so-called aromaticity. When a metal atom is bound to the benzene ring, charge transfer takes place, and the benzene becomes highly electron-rich. If a benzene molecule is bound by two Ba atoms, the benzene has 10π electrons (Figure 4a).[39] The ground state of the benzene complex is the singlet state, while the first and second excited states are the triplet and quintet spin states, respectively.

When an electric field is applied to this complex (either perpendicular or parallel to the benzene ring plane), the MO energy levels are changed due to the second-order Stark effect. The excited states have higher polarizability than the singlet ground state. Then, above a certain threshold field, the ground state changes to a triplet state due to the energy level crossing between the ground state and excited states as shown in Figure 4b. Thus, in a weak electric field, the ground state of the complex is a nonmagnetic singlet state, whereas above a certain threshold electric field, it becomes a magnetic triplet state. That is, magnetic on/off switching is possible with electric fields. This exotic phenomenon can be observed if a molecule has a nonmagnetic ground state and a magnetic excited state of high polarizability whose energy is only slightly above the ground state energy.[40]

Figure 4c shows a two-terminal device comprised of a magnetic switching molecule connected to two metal electrodes, which can apply an electric bias across the device. In this device, the bias voltage not only drives electrical currents through the molecule but also changes the magnetic state of the molecule as it increases over a certain threshold value, which means that one does not need to employ a magnet as the third gate to switch on the molecular magnetic state. This would lead to high density devices.

Effect of a Magnetic Field on Molecular Orbitals

An external magnetic field must be a useful means to manipulate the magnetic structure of a molecular system. The interaction between a magnetic dipole moment ($\boldsymbol{\mu}_{\text{m}}$) and applied magnetic field (**B**) gives an additional energy term in the Hamiltonian:

$$\Delta\varepsilon = -\boldsymbol{\mu}_{\text{m}} \cdot \mathbf{B} \tag{6}$$

This term leads to shift of energy levels according to their spin dipole moments ($\boldsymbol{\mu}_{\text{m}} = g\mu_{\text{B}}\mathbf{S}$, where g is the Landé g-fac-

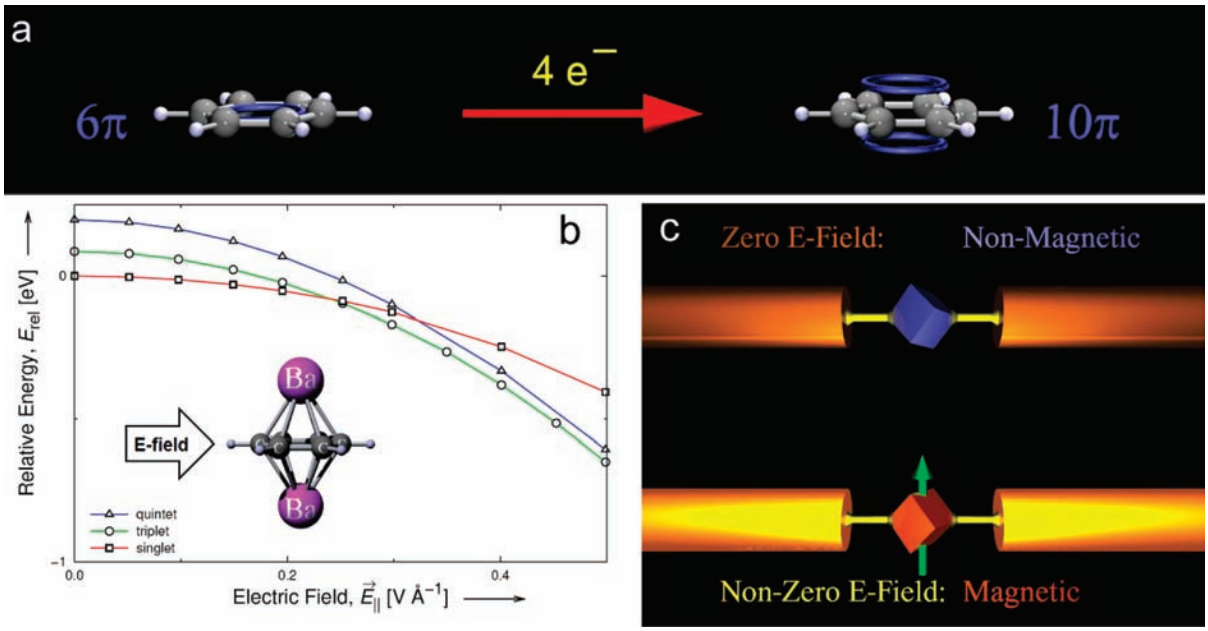

FIGURE 4. (a) An electron-rich form of benzene with 10π electrons. (b) Stark effect on the relative energies of the singlet (□), triplet (○), and quintet (△) electronic spin states in high-electron-density benzene. (c) Electric field driven magnetic switching device.[39]

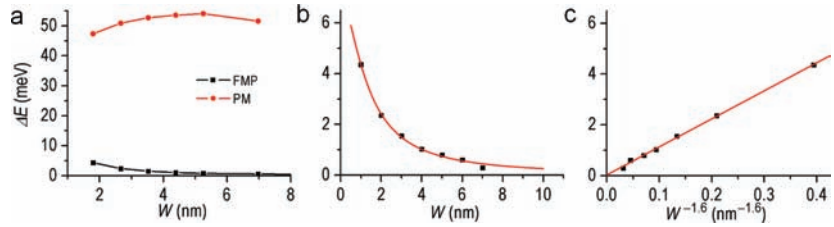

FIGURE 5. Energy difference between ferromagnetic parallel (FMP), ferromagnetic antiparallel (FMA), and paramagnetic (PM) configurations for various widths of the ZGNR: (a) relative energy per edge atom of the FMP/PM configurations with respect to the FMA configuration for various widths; (b) power-law and (c) linear fittings of the energy difference between FMP and FMA for various widths. The exponent in the power-law is −1.6.[57]

tor, μ_B is the Bohr magneton, and **S** is a vector of the spin magnetic moment), which is called the Zeeman effect. Application of very strong magnetic fields to the molecular system induces noticeable modulations of conductance with change of the electron's phase due to the Aharonov−Bohm effect.[41−43] However, in this section, we introduce a more exotic and intriguing role of a magnetic field in a nanodevice than the usual case.

A graphene nanoribbon (GNR) denotes a nanometer-scale strip of a graphene that is a sheet of graphite.[44,45] This novel nanostructure has many intriguing properties to be utilized in nanomaterial science.[46−50] Especially, many efforts have been devoted to investigating the magnetic structure of the GNR with zigzag-shape edges (ZGNR).[51−57] It has been known that the ZGNR has a ferromagnetic spin ordering along both edges. The relative spin orientation between both edges can be either parallel or antiparallel. The parallel spin configuration (ferromagnetic parallel, FMP) has slightly higher energy than the antiparallel spin configuration (ferromagnetic antiparallel, FMA). For example, a ZGNR with ∼4 nm width shows ∼1 meV energy difference based on density functional theory using the functional of Perdew, Burke, and Ernzerhof (Figure 5).[58] Although the energy difference slightly varies depending on the functional employed,[59] it shows a power law as a function of the width of the ribbon, as depicted in Figure 5.[57] In the presence of an external magnetic field, however, the FMP state should be the energetic-minimum structure, since spin magnetic moments favor the parallel direction with the applied magnetic field due to the energy gain shown in eq 6.

Herein, we only focus on the FMP state, that is, the parallel spin configuration between both edges. Figure 6 exhibits the band structure of the 8-ZGNR (*N*-ZGNR denotes a ZGNR with *N* zigzag chains) and its corresponding orbital symmetries. The occupied bands below the Fermi energy (E_F) have C_2

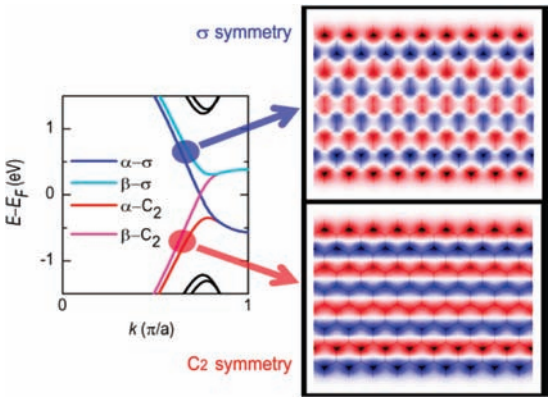

FIGURE 6. Orbital symmetries of the band structure of the 8-ZGNR. The upper and lower panels on the right exhibit the orbitals (wave functions) corresponding to the blue/cyan and red/pink bands on the left panel, respectively. The upper panel shows σ symmetry with respect to the middle horizontal line, while the lower panel shows C_2 symmetry.[57]

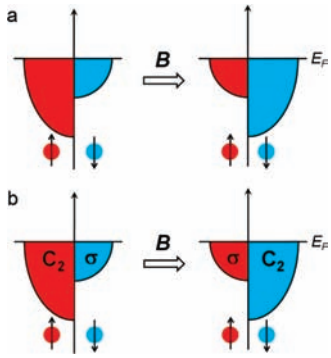

FIGURE 7. Schematic representations of densities of states (DOS) for a usual ferromagnetic metal (a) and the ferromagnetic state of a ZGNR (b). For the usual ferromagnetic metal, the spin symmetries in the DOS are changed by the applied magnetic field, while for the ZGNR, spin symmetries, as well as their orbital symmetries, in the DOS are simultaneously switched.

symmetry regardless of their spins, while the unoccupied bands have "σ" symmetry. Thus, both occupied and unoccupied bands have orbital symmetries orthogonal to each other. More interestingly, one can change the spin polarization of the occupied bands by applying magnetic fields. As a result, for the same spins, their orbital symmetries become orthogonal. This is quite an unusual behavior, compared with the magnetic control of the spin polarization in usual ferromagnetic materials. Figure 7 clearly shows their difference. Figure 7a presents typical switching behavior of the spin polarization due to the magnetic field in the density of states (DOS) of a usual ferromagnetic metal, while Figure 7b exhibits switching behavior of both spin polarization and orbital symmetries in the DOS of a ZGNR. Consequently, for ZGNRs, their orbital symmetries as well as the spin symmetries can be manipulated by magnetic control. In the following section, we show how this novel property of the ZGNR is exploited in spintronics.

Super Magnetoresistance in ZGNR Spin-Valve Devices

As an application of the magnetic property of a ZGNR, we have investigated characteristics of a spin-valve device based on ZGNRs.[57] Figure 8 shows the proposed structure of the spin-valve device. A ZGNR is placed between two ferromagnetic (FM) electrodes whose magnetic fields control the spin orientation of the ZGNR, analogous to the prototype of conventional spin-valve devices (FM−spacer−FM). However, the difference is that conventional spin-valve devices of giant or tunneling magnetoresistance (GMR[60−62] or TMR[63−65]) usually employ a nonmagnetic metal (NM) or insulator (I) as a spacer (FM−NM−FM or FM−I−FM), while in the present case of super-magnetoresistance (SMR), the ferromagnetic ZGNR is employed as a spacer (FM−FM−FM). This distinction eventually gives rise to an extreme enhancement in the spin-valve effect compared with conventional devices, due to the novel mechanism, which is completely different from the conventional one.

In Figure 8, if the directions of magnetic fields at both FM electrodes are parallel, the spin polarizations of a ZGNR will be uniform, whereas if the directions are antiparallel, the spin polarizations at both sides of the ZGNR will be antiparallel with the formation of a magnetic domain wall between them. This causes spin-dependent conductance or resistance through the ZGNR device.

Figure 9 shows a conceptual mechanism of the spin-dependent resistance for conventional and ZGNR spin-valve devices. The mechanism of the spin-dependent resistance in spin-valve devices depends on the type of the spacer material, since it plays a role as a medium in the spin-transfer process occurring between two FM electrodes. In the conventional case, we have small resistance for the parallel spins due to the large values of the up-spin DOS at both sides but large resistance for antiparallel spins due to the small values of the DOS at least at one side. Thus, the spin-dependent resistance is mainly determined by matching of the spin-polarized DOS in the two FM electrodes. By definition, the effectiveness of a spin-valve device is given by the relative ratio (magnetoresistance ratio, MR) between the resistances for parallel and antiparallel spin configurations (R_P and R_{AP}, respectively):

$$\mathrm{MR} \equiv \frac{G_P - G_{AP}}{G_{AP}} = \frac{R_{AP} - R_P}{R_P} \qquad (7)$$

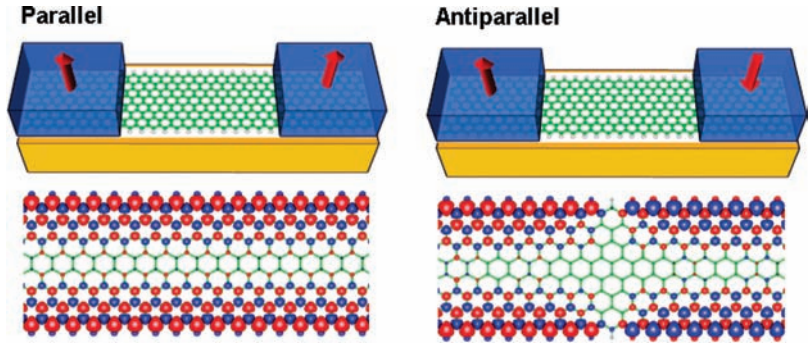

FIGURE 8. Schematic ZGNR-based spin-valve device with parallel and antiparallel spin configurations and the corresponding spin-magnetization density isosurfaces. The blue boxes represent ferromagnetic electrodes to control spin polarization of the ZGNR device, and the red arrows indicate the directions of applied magnetic fields. In the isosurfaces, red/blue color denotes up/down spin and a ZGNR skeleton is drawn in green color.[57]

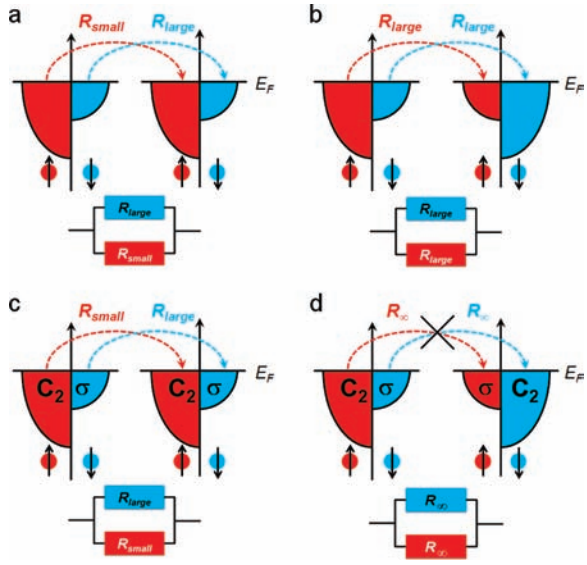

FIGURE 9. Spin-transfer paths from the left to right densities of states of the ferromagnetic leads for (a) parallel and (b) antiparallel spin configurations in a conventional spin-valve device and for (c) parallel and (d) antiparallel spin configurations in a ZGNR spin-valve device.

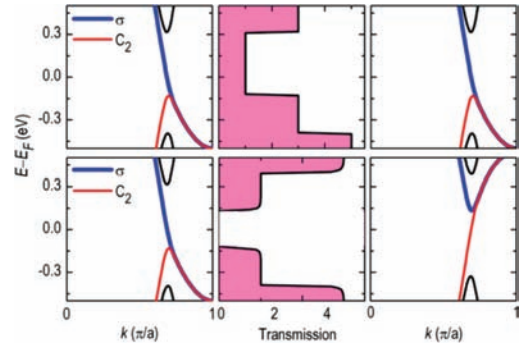

FIGURE 10. Band structure for the left lead (left), transmission curve (middle), and band structure for the right lead (right) for the α-spin in the parallel (upper panel) and antiparallel (lower panel) configurations of the 32-ZGNR at zero bias.[57]

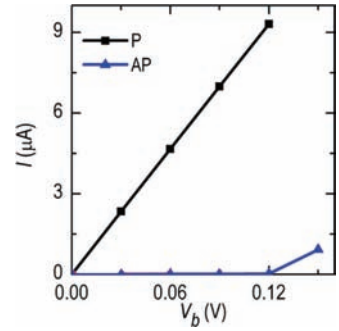

FIGURE 11. *I*−*V* curves of the 32-ZGNR spin-valve device for the parallel (P) configuration (black) and the antiparallel (AP) configuration (blue) at 5 K.[57]

where G_P and G_{AP} are the conductance value for the parallel and antiparallel spin configurations.

For a ZGNR spin-valve device, the DOS in each spin configuration has additional labels denoting the orbital symmetry of the spin state that is discussed in the previous section. Therefore, spin-dependent resistance and thereby MR are determined by not only the spin matching but also the orbital symmetry matching in the DOS structures. As a result, spin transfer for the antiparallel spin configuration is not allowed due to mismatching between the orbital symmetries at both sides, which could lead to an ideal spin valve with infinite MR value in eq 7.

To quantitatively investigate the surprising phenomenon, we have calculated transmission values and currents of the ZGNR spin-valve device at the first-principles level. Figure 10 exhibits the transmission curves sandwiched by band structures at the left and right leads for the ZGNR (only for the case of the up (α) spin to avoid complexity). The blue and red lines represent the corresponding orbitals that have the C_2 and σ symmetries, respectively. For the parallel case, bands having the same symmetry are aligned for all energy ranges, yielding perfect transmission (upper panel in Figure 10). In contrast, for the antiparallel case, the transmission curve has perfect reflection, resulting in zero transmission values within

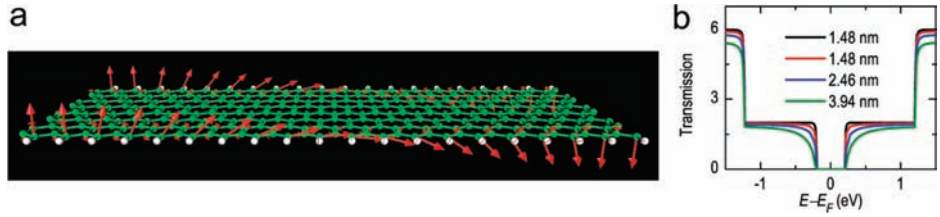

FIGURE 12. (a) The noncollinear spin orientations in a domain wall of the 8-ZGNR for the antiparallel case and (b) transmission curves depending on the domain wall size. The black line is for the collinear spin configuration, while the others are for the noncollinear spin configurations.[57]

a particular energy range around the E_F where the orbital symmetries are mismatching (lower panel in Figure 10).

Figure 11 shows the calculated $I-V$ characteristics for the 32-ZGNR spin-valve device using eq 1. For the parallel spin configuration, it shows a linear curve with a specific slope corresponding to the quantized conductance ($2e^2/h$), as a consequence of the perfect transmission values at the E_F. In contrast, for the antiparallel spin configuration, the current is suppressed below a certain threshold voltage, resulting in huge resistance. In this way, the MR value of the ZGNR device at low temperature exceeds a million percent, which rapidly approaches infinity as the temperature goes to zero. The temperature effect is taken into account by the Fermi distribution function in eq 1. Indeed, double spin-filtering effect opens a new way toward an ideal spin-valve device with a new type of MR, so-called SMR.

Here, in the case of the antiparallel spin configuration, we need to address the effect of a magnetic domain wall, which is formed between two ferromagnetic leads in the ZGNR devices as shown in Figure 12a. To this end, we have calculated the transmission function with various domain wall sizes in the noncollinear spin-polarized mode.[57] In Figure 12b, transmissions for the noncollinear spin states result in reduced sharpness of corners in the curves depending on the domain wall size; the thicker the domain wall is, the more rounded the curve is. However, the zero transmission regions leading to the infinite resistance at a low bias are not affected by the domain wall size. Consequently, the conclusion based on the collinear spin state should be the same as that based on the noncollinear spin state.

Conclusions

Molecular orbitals (MOs) play a central role for quantum transport in molecular electronic and spintronic devices. Thus, manipulation of the MOs is a direct way to tune transport properties of a molecule for the design of interactive devices. An electric field is a powerful means to change energy and shape of MOs. Owing to the quadratic Stark effect, a particular MO with high polarizability can be distinctively influenced by the field. We have shown that using this effect, one can make an electric field-driven magnetic switching device without a strong magnet as the third gate. On the other hand, an external magnetic field changes not only spin polarization but also orbital symmetry in the case of ferromagnetic graphene nanoribbons. This unusual effect enables us to design a novel spintronic device. For instance, a spin-valve device based on graphene nanoribbons shows exotic super-magnetoresistance with new mechanism: doubling the filtering effect through orbital symmetry matching as well as spin matching. This opens a new pathway toward an ideal spin-valve device.

To date, the MO theory has been used as a universal language in quantum chemistry to explain chemical reactions, molecular properties, structures, and so on. The language is also useful to the new field exploring transport properties of a molecule. Investigating the role of MOs is a starting point to understand complicated quantum phenomena in molecular electronics and spintronics. Its first step is a systematic study: (1) change of conductance depending on the feature of MOs including their shape and symmetry, (2) change of MOs by substitution of functional groups, and (3) change of MOs due to the metal−molecule junctions. The next step is to appropriately tune the MOs with external fields to control the conductance of a molecular device on the basis of understanding the influence of fields on MOs. We believe that such efforts offer intuitive approaches to the design of novel molecular electronic devices and eventually realize practical and interactive molecular devices.

This work was supported by GRL (KICOS), KOSEF (WCU, R32-2008-000-10180-0; EPB Center, R11-2008-052-01000), and BK21(KRF).

BIOGRAPHICAL INFORMATION

Woo Youn Kim was born in Gyeongsan, Korea, in 1978. He received his Ph.D. degree in chemistry from Pohang University of Science and Technology (POSTECH) for research on electron and spin transport phenomena in nanodevices under the guidance of Prof. Kwang S. Kim in 2009. In 2008, he was a visiting scientist at the Freie Universität Berlin in Germany. He is now a postdoc-

toral fellow in Prof. Kim's lab at POSTECH. His research interest focuses on development of new theoretical methods for applications to molecular electronics and spintronics.

Kwang S. Kim was born in Seoul, Korea, in 1950. He received his Ph.D. degree from University of California, Berkeley. He was a postdoctoral fellow at IBM and a visiting scientist at Rutgers University, MIT, and Columbia University. Currently, he is a professor in the Department of Chemistry and the director of the Center for Superfunctional Materials at Pohang University of Science and Technology. His research interests include design and development of novel nanomaterials and molecular devices.

FOOTNOTES

*To whom correspondence should be addressed. E-mail address: kim@postech.ac.kr.

REFERENCES

1 Aviram, A.; Ratner, M. A. Molecular rectifiers. *Chem. Phys. Lett.* **1974**, *29*, 277–283.

2 Tao, N. J. Electron transport in molecular junctions. *Nat. Nanotechnol.* **2006**, *1*, 173–181.

3 Chem, F.; Hihath, J.; Huang, Z.; Li, X.; Tao, N. J. Measurement of single-molecule conductance. *Annu. Rev. Phys. Chem.* **2007**, *58*, 535–564.

4 Guo, X.; Small, J. P.; Klare, J. E.; Wang, Y.; Purewal, M. S.; Tam, I. W.; Hong, B. H.; Caldwell, R.; Huang, L.; O'Brien, S.; Yan, J; Breslow, R.; Wind, S. J.; Hone, J.; Kim, P.; Nuckolls, C. Covalently bridging gaps in single-walled carbon nanotubes with conducting molecules. *Science* **2006**, *311*, 356–359.

5 Feldman, A. K.; Steigerwald, M. L.; Guo, X.; Nuckolls, C. Molecular electronic devices based on single-walled carbon nanotube electrodes. *Acc. Chem. Res.* **2008**, *41*, 1731–1741.

6 Nitzan, A.; Ratner, M. A. Electron transport in molecular wire junctions. *Science* **2003**, *300*, 1384–1389.

7 Galperin, M.; Ratner, M. A.; Nitzan, A.; Troisi, A. Nuclear coupling and polarization in molecular transport junctions: Beyond tunneling to function. *Science* **2008**, *319*, 1056–1060.

8 Kim, W. Y.; Choi, Y. C.; Min, S. K.; Cho, Y.; Kim, K. S. Application of quantum chemistry to nanotechnology: Electron and spin transport in molecular devices. *Chem. Soc. Rev.* **2009**, *38*, 2319–2333.

9 Kim, W. Y.; Choi, Y. C.; Kim, K. S. Understanding structures and electronic/spintronic properties of single molecules, nanowires, nanotubes, and nanoribbons towards the design of nanodevices. *J. Mater. Chem.* **2008**, *18*, 4510–4521.

10 Metzger, R. M. Unimolecular electronics. *J. Mater. Chem.* **2008**, *18*, 4364–4396.

11 Chen, F.; Tao, N. J. Electron transport in single molecules: From benzene to graphene. *Acc. Chem. Res.* **2009**, *42*, 429–438.

12 Avouris, P.; Chen, Z.; Perebeinos, V. Carbon-based electronics. *Nat. Nanotechnol.* **2007**, *2*, 605–615.

13 Majumdar, D.; Lee, H. M.; Kim, J.; Kim, K. S. Photoswitch and nonlinear optical switch: Theoretical studies on 1,2-bis-(3-thienyl) - ethene derivatives. *J. Chem. Phys.* **1999**, *111*, 5866–5872.

14 Datta, S. *Electronic Transport in Mesoscopic Systems*; Cambridge University Press: Cambridge, England, 1995;Chapter 3.

15 Ventra, M. D.; Pantelides, S. T.; Lang, N. D. First-principles calculation of transport properties of a molecular device. *Phys. Rev. Lett.* **2000**, *84*, 979.

16 Taylor, J.; Guo, H.; Wang, J. Ab initio modeling of quantum transport properties of molecular electronic devices. *Phys. Rev. B* **2001**, *63*, 245407.

17 Brandbyge, M.; Mozos, J.-L.; Ordejon, P.; Taylor, J.; Stokbro, K. Density-functional method for nonequilibrium electron transport. *Phys. Rev. B* **2002**, *65*, 165401.

18 Palacios, J. J.; Perez-Jimenez, A. J.; Louis, E.; Verges, J. A. Fullerene-based molecular nanobridges: A first-principles study. *Phys. Rev. B* **2001**, *64*, 115411.

19 Ke, S.-H.; Baranger, H. U.; Wang, W. Electron transport through molecules: Self-consistent and non-self-consistent approaches. *Phys. Rev. B* **2004**, *70*, 085410.

20 Kim, Y.-H.; Tahir-Kheli, J.; Schultz, P. A.; Goddard, W. A., III. First-principles approach to the charge-transport characteristics of monolayer molecular-electronics devices: Application to hexanedithiolate devices. *Phys. Rev. B* **2006**, *73*, 235419.

21 Rocha, A. R.; Garcia-Suarez, V. M.; Bailey, S. W.; Lambert, C. J.; Ferrer, J.; Sanvito, S. Spin and molecular electronics in atomically generated orbital landscapes. *Phys. Rev. B* **2006**, *73*, 085414.

22 Kurth, S.; Stefanucci, G.; Almbladh, C.-O.; Rubio, A.; Gross, E. K. U. Time-dependent quantum transport: A practical scheme using density functional theory. *Phys. Rev. B* **2005**, *72*, 035308.

23 Thygesen, K. S.; Rubio, A. Nonequilibrium GW approach to quantum transport in nano-scale contacts. *J. Chem. Phys.* **2007**, *126*, 091101.

24 Kim, W. Y.; Kim, K. S. Carbon nanotube, graphene, nanowire, and molecule-based electron and spin transport phenomena using the nonequilibrium Green's function method at the level of first principles theory. *J. Comput. Chem.* **2008**, *29*, 1073–1083.

25 Fisher, D. S; Lee, P. A. Relation between conductivity and transmission matrix. *Phys. Rev. B* **1981**, *23*, 6851–6854.

26 Soler, J. M.; Artacho, E.; Gale, J. D.; García, A.; Junquera, J; Ordejón, P.; Sánchez-Portal, D. The SIESTA method for ab initio order-N materials simulation. *J. Phys.: Condens. Matter* **2002**, *14*, 2745–2779.

27 Hall, L. E.; Reimers, J. R.; Hush, N. S.; Silverbrook, K. Formalism, analytical model and a priori-Green's function-based calculations of the current-voltage characteristics of molecular wires. *J. Chem. Phys.* **2000**, *112*, 1510–1521.

28 Ahn, C. H.; Triscone, J.-M.; Mannhart, J. Electric field effect in correlated oxide systems. *Nature* **2003**, *424*, 1015–1018.

29 Ahn, C. H.; Gariglio, S.; Paruch, P.; Tybell, T.; Antognazza, L.; Triscone, J.-M. Electrostatic modulation of superconductivity in ultra-thin $GdBa_2Cu_3O_7$ films. *Science* **1999**, *284*, 1152–1155.

30 Son, Y.-W.; Cohen, M. L.; Louie, S. G. Electric field effects on spin transport in defective metallic carbon nanotubes. *Nano Lett.* **2007**, *7*, 3518–3522.

31 Ventra, M. D.; Pantelides, S. T.; Lang, N. D. The benzene molecule as a molecular resonant-tunneling transistor. *Appl. Phys. Lett.* **2000**, *76*, 3448–3450.

32 Ghosh, A. W.; Rakshit, T.; Datta, S. Gating of a molecular transistor: Electrostatic and conformational. *Nano Lett.* **2004**, *4*, 565–568.

33 Hod, O.; Baer, R.; Rabani, E. A parallel electromagnetic molecular logic gate. *J. Am. Chem. Soc.* **2005**, *127*, 1648–1649.

34 Perrine, T. M.; Smith, R. G.; Marsh, C.; Dunietz, B. D. Gating of single molecule transistors: Combining field-effect and chemical control. *J. Chem. Phys.* **2008**, *128*, 154706.

35 Choi, Y. C.; Kim, W. Y.; Park, K.-S.; Tarakeshwar, P.; Kim, K. S. Role of molecular orbitals of the benzene in electronic nanodevices. *J. Chem. Phys.* **2005**, *122*, 094706.

36 Žutić, I.; Fabian, J.; Sarma, S. D. Spintronics: Fundamentals and applications. *Rev. Mod. Phys.* **2004**, *76*, 323–410.

37 Sahoo, S.; Kontos, T.; Furer, J.; Hoffmann, C.; Gräber, M.; Cottet, A.; Schönenberger, C. Electric field control of spin transport. *Nat. Phys.* **2005**, *1*, 99–102.

38 Mi, Y.; Zhang, M.; Yana, H. Effect of electric-field on spin transport and spin current in an organic semiconductor system. *Phys. Lett. A* **2008**, *372*, 6434–6437.

39 Diefenbach, M.; Kim, K. S. Towards molecular magnetic switching with an electric bias. *Angew. Chem., Int. Ed.* **2007**, *46*, 7640–764.

40 Misiorny, M; Barnaś, J. Effects of intrinsic spin-relaxation in molecular magnets on current-induced magnetic switching. *Phys. Rev. B* **2008**, *77*, 172414.

41 Bachtold, A; Strunk, C.; Salvetat, J.-P.; Bonard, J.-M.; Forró, L.; Nussbaumer, T.; Schönenberger, C. Aharonov-Bohm oscillations in carbon nanotubes. *Nature* **1999**, *397*, 673–675.

42 Hod, O.; Rabani, E; Baer, R. Magnetoresistance of nanoscale molecular devices. *Acc. Chem. Res.* **2006**, *39*, 109–117.

43 Lassagne, B.; Cleuziou, J.-P.; Nanot, S.; Escoffier, W.; Avriller, R.; Roche, S.; Forró, L.; Raquet, B.; Broto, J.-M. Aharonov-Bohm conductance modulation in ballistic carbon nanotubes. *Phys. Rev. Lett.* **2007**, *98*, 176802.

44 Novoselov, K. S.; Geim, A. K.; Morozov, S. V.; Jiang, D.; Zhang, Y.; Dubonos, S. V.; Grigorieva, I. V.; Firsov, A. A. Electric field effect in atomically thin carbon films. *Science* **2004**, *306*, 666–669.

45 Kim, K. S.; Zhao, Y.; Jang, H.; Lee, S. Y.; Kim, J. M.; Kim, K. S.; Ahn, J.-H.; Kim, P.; Choi, J.-Y.; Hong, B. H. Large-scale pattern growth of graphene films for stretchable transparent electrodes. *Nature* **2009**, *457*, 706–710.

46 Neto, A. H. C.; Guinea, F.; Peres, N. M. R.; Novoselov, K. S.; Geim, A. K. The electronic properties of graphene. *Rev. Mod. Phys.* **2009**, *81*, 109–162.

47 Li, X.; Wang, X.; Zhang, L.; Lee, S.; Dai, H. Chemically derived, ultrasmooth graphene nanoribbon semiconductors. *Science* **2008**, *319*, 1229–1232.

48 Kosynkin, D. V.; Higginbotham, A. L.; Sinitskii, A.; Lomeda, J. R.; Dimiev, A.; Price, B. K.; Tour, J. M. Longitudinal unzipping of carbon nanotubes to form graphene nanoribbons. *Nature* **2009**, *458*, 872–876.

49 Jiao, L.; Zhang, L.; Wang, X.; Diankov, G.; Dai, H. Narrow graphene nanoribbons from carbon nanotubes. *Nature* **2009**, *458*, 877–880.

50 Jia, X.; Hofmann, M.; Meunier, V.; Sumpter, B. G.; Campos-Delgado, J.; Romo-Herrera, J. M.; Son, H.; Hsieh, Y.-P.; Reina, A.; Kong, J.; Terrones, M.; Dresselhaus, M. S. Controlled formation of sharp zigzag and armchair edges in graphitic nanoribbons. *Science* **2009**, *323*, 1701–1705.

51 Nakada, K.; Fujita, M.; Dresselhaus, G.; Dresselhaus, M. S. Edge state in graphene ribbons: Nanometer size effect and edge shape dependence. *Phys. Rev. B* **1996**, *54*, 17954–17961.

52 Son, Y.-W.; Cohen, M. L.; Louie, S. G. Half-metallic graphene nanoribbons. *Nature* **2006**, *444*, 347–349.

53 Hod, O.; Barone, V.; Peralta, J. E.; Scuseria, G. E. Enhanced half-metallicity in edge-oxidized zigzag graphene nanoribbons. *Nano Lett.* **2007**, *7*, 2295–2299.

54 Pisani, L.; Chan, J. A.; Montanari, B.; Harrison, N. M. Electronic structure and magnetic properties of graphitic ribbons. *Phys. Rev. B* **2007**, *75*, 064418.

55 Choi, S.-M.; Jhi, S.-H. Self-assembled metal atom chains on graphene nanoribbons. *Phys. Rev. Lett.* **2008**, *101*, 266105.

56 Munoz-Rojas, F.; Fernandez-Rossier, J.; Palacios, J. J. Giant magnetoresistance in ultrasmall graphene based devices. *Phys. Rev. Lett.* **2009**, *102*, 136810.

57 Kim, W. Y.; Kim, K. S. Prediction of very large values of magnetoresistance in a graphene nanoribbon device. *Nat. Nanotechnol.* **2008**, *3*, 408–412.

58 Perdew, J. P.; Burke, K.; Ernzerhof, M. Generalized gradient approximation made simple. *Phys. Rev. Lett.* **2006**, *77*, 3865–3868.

59 Hod, O.; Barone, V.; Scuseria, G. E. Half-metallic graphene nanodots: A comprehensive first-principles theoretical study. *Phys. Rev. B* **2008**, *77*, 035411.

60 Binasch, G.; Grunberg, P.; Saurenbach, F.; Zinn, W. Enhanced magnetoresistance in layered magnetic structures with antiferromagnetic interlayer exchange. *Phys. Rev. B* **1989**, *39*, 4828–4830.

61 Baibich, M. N.; Broto, J. M.; Fert, A.; Van Dau, F. N.; Petro, F.; Etienne, P.; Creuzet, G.; Friederich, A.; Chazelas, J. Giant magnetoresistance of (001)Fe/(001)Cr magnetic superlattices. *Phys. Rev. Lett.* **1988**, *61*, 2472–2475.

62 Parkin, S. S. P.; More, N.; Roche, K. P. Oscillations in exchange coupling and magnetoresistance in metallic superlattice structures: Co/Ru, Co/Cr, and Fe/Cr. *Phys. Rev. Lett.* **1990**, *64*, 2304–2307.

63 Julliere, M. Tunneling between ferromagnetic films. *Phys. Lett. A* **1975**, *54*, 225–226.

64 Yuasa, S.; Nagahama, T.; Fukushima, A.; Suzuki, Y.; Ando, K. Giant room-temperature magnetoresistance in single-crystal Fe/MgO/Fe magnetic tunnel junctions. *Nat. Mater.* **2004**, *3*, 868–871.

65 Parkin, S. S. P.; Kaiser, C.; Panchula, A.; Rice, P. M.; Hughes, B.; Samant, M.; Yang, S.-H. Giant tunnelling magnetoresistance at room temperature with MgO (100) tunnel barriers. *Nat. Mater.* **2004**, *3*, 862–867.